ELSEVIER

Earth and Planetary Science Letters 152 (1997) 163–180

EPSL

# Determining the burial time of single grains of quartz using optically stimulated luminescence

Andrew S. Murray [a,*], Richard G. Roberts [b,1]

[a] *CSIRO Division of Water Resources, P.O. Box 1666, Canberra, ACT 2601, Australia*
[b] *School of Earth Sciences, La Trobe University, Melbourne, VIC 3083, Australia*

Received 9 March 1997; revised 29 August 1997; accepted 6 September 1997

**Abstract**

In the optical dating of sediments it is usually assumed that the optically stimulated luminescence (OSL) signal has been completely reset by light exposure prior to burial; this assumption is often not valid. One approach to testing, and perhaps circumventing, this assumption is to examine the apparent date of last exposure to daylight of individual sediment grains. This paper reports on the application, for the first time, of 2 new measurement protocols to the estimation of the radiation dose received during burial for individual quartz grains from an aeolian deposit of known age (10,000 year old), which is considered likely to have been completely reset by sunlight at deposition. Additive-dose (laboratory doses added to the burial dose before OSL measurement) and regenerative-dose (doses added after measurement of OSL from burial dose) single-aliquot protocols are applied to 28 and 25 individual grains, respectively; each grain provides an independent estimate ($D_e$) of the burial dose. The average $D_e$ from the additive-dose protocol ($21.8 \pm 1.1$ Gy) is in good agreement with the average from the regenerative-dose protocol ($23.8 \pm 1.0$ Gy). Both agree well with: (1) 13 multiple-grain regenerative-dose single-aliquot measurements, each on 1 mg sub-samples, of $23.9 \pm 0.3$ Gy; (2) 9 multiple-grain additive-dose single-aliquot measurements, also on 1 mg sub-samples, of $22.4 \pm 0.7$ Gy; and (3) one previously published multiple-aliquot additive-dose estimate of $23.5 \pm 0.6$ Gy using 52 sub-samples, each of 5 mg. The resulting optical ages are in good accord with $^{14}C$ and thermoluminescence age determinations. The distribution of equivalent doses in the single grains is, however, unexpectedly large ($\sigma \approx 23\%$ of mean $D_e$), given the very likely complete resetting of the OSL signal at deposition. Possible reasons are discussed, and it is concluded that heterogeneity in beta dosimetry is the most likely explanation. The single-grain optical dating protocols reported here allow a detailed examination of the dose distribution in very small samples. Thus, they should enable accurate dates to be obtained for sediments and soils that contain poorly bleached or mixed-age components, as well as deposits in which quartz grains are present in extremely low abundance. © 1997 Elsevier Science B.V.

*Keywords:* luminescence; eolianite; quartz; grains

* Corresponding author. Present address: The Nordic Laboratory for Luminescence Dating, Risø National Laboratory, DK-4000 Roskilde, Denmark. Fax: +45 46 77 46 07.

[1] Fax: +61 3 9479 1272. E-mail: bert.roberts@latrobe.edu.au


*PII* S0012-821X(97)00150-7

## 1. Introduction

To see a World in a Grain of Sand
And a Heaven in a Wild Flower
Hold Infinity in the palm of your hand
And Eternity in an hour

(William Blake, from *Auguries of Innocence*, ca. 1803).

The ability to obtain age estimates from single grains of sand has eluded luminescence dating methods. Over the past decade, other geochronological methods have progressed towards analysis of very small samples, such as single crystals in $^{40}Ar/^{39}Ar$ dating [1], individual amino acids in accelerator mass spectrometry $^{14}C$ dating [2], and sample masses of $< 100$ mg for thermal ionisation mass spectrometry $^{230}Th/^{234}U$ analyses [3]. A major advantage of decreasing sample size is the ability to identify the presence of contaminants in a bulk sample, and to exclude them from the final age determination. In luminescence dating, protocols required to analyse a true single-aliquot of sample have only just been devised for feldspars [4] and quartz [5]. In principle, these permit age estimates to be obtained for individual grains of these ubiquitous minerals in Quaternary sedimentary deposits. Here we describe the novel application of two optical dating protocols to single grains of quartz sand and present surrogate age frequency distributions for single grains extracted from a 10 ka (1 ka = 1000 yr) aeolian deposit in southern Australia.

Huntley et al. [6] first proposed optical dating as the natural extension of the thermoluminescence (TL) procedures which Wintle and Huntley [7] had developed for dating sedimentary materials. Optically stimulated luminescence (OSL) is especially appropriate for the dating of wind-blown and water-lain sediments because it preferentially samples electrons held in light-sensitive traps. These traps are most likely to have been emptied by exposure to sunlight ('bleached') during sediment transport, and so be effectively reset at the time of deposition. The dose absorbed subsequently from the environmental ionising–radiation field will then be proportional to the time since deposition. An OSL signal which increases with this dose is measured by a controlled exposure of the sample to light in the laboratory, during which electrons are again excited from the light-sensitive traps. UV and visible photons are emitted during the recombination of a proportion of these excited electrons, and these photons can be discriminated from the stimulating light source with appropriate optical filters.

Protocols for the luminescence dating of sediments, using TL or OSL, have until recently required a theoretical minimum of two sub-samples of the material to be dated; practical analyses usually involve the measurement of several tens of sub-samples ([6,8]). It has been a necessary assumption that these sub-samples have identical luminescence characteristics, and an identical history of exposure to light and to the natural radiation environment; we refer to such sub-samples as aliquots. Such measurement-intensive procedures have obvious practical limitations in terms of sample size and instrument time; they also have more fundamental limitations when the requirement for aliquots cannot be met, for instance when the material is inherently heterogeneous. Such heterogeneity has been reported in both feldspars and quartz by several authors [9–14], and techniques for recognising such samples have been suggested [10,14,15]. Murray et al. [12] and Olley et al. [13] examined this heterogeneity in more detail using a simplified technique for estimating $D_e$. They measured the natural OSL signal (i.e. the signal observed without giving a laboratory radiation dose), gave the same sample a known beta dose to regenerate the OSL, and then used the ratio of the natural to the regenerated OSL to estimate the natural dose. (The laboratory dose which gives rise to a luminescence signal equal to the natural signal is known as the equivalent dose, $D_e$.) They acknowledged that this protocol may have inherent weaknesses and was only suitable for very young samples but it allowed them to examine the distribution of dose in aliquots from a single sample. They studied fluvially transported sediments that were either known to be recently transported, or were $< 200$ years old. By examining small samples, of only a few tens or hundreds of grains, they were able to conclude that the majority of grains had been well bleached during transport, but that there was a small number of poorly bleached grains present. These 'contaminating' grains gave rise to an average $D_e$ in modern samples that was consistent with an age of up to

several thousand years. However, the dose in the few sub-samples made up entirely of well bleached grains was consistent with the true time since deposition.

Sediments transported and deposited in other environmental settings are expected to display similar heterogeneity in luminescence characteristics. Coastal storm and tsunami-laid deposits [16] are apt to be poorly or variably bleached, as are colluvial and mass movement deposits [10,17] and glaciofluvial sediments [11,14]. In such instances, valuable chronological information could be extracted if the dose distribution was measured on a grain-by-grain basis. Incompletely bleached grains could be identified and rejected from the age calculation procedure, resulting in more accurate age estimates than could be obtained using the average dose. Lamothe et al. [9] attempted to date large single grains of feldspar from marine sands; they concluded that both anomalous fading [18] and incomplete bleaching contributed to their dose distributions, precluding reliable age estimates. The ability to date single grains would be of considerable value in studies of soil formation and disturbance, such as mixing by bioturbation [15] and the development of pedogenic carbonates [19]. At archaeological sites, single-grain dating would permit discrimination between grains that had been completely bleached at deposition and, in the worst case, grains liberated by the in situ disintegration of buried rubble or weathered bedrock; the latter grains would not have been exposed to sunlight since the time of rock formation.

Analysis of individual grains should be especially valuable when sample mass is restricted and a 'microstratigraphic' approach is desired. For example, quartz grains removed from the surface rind and successively deeper layers of a mud-wasp nest were used to check that the core of the nest contained concealed grains suitable for optical dating [20]. A similar strategy might be used to date grains trapped in or beneath rock varnish and other precipitate crusts. Richards [21] took a microstratigraphic approach to extract quartz grains from the previously light-exposed portions of buried quartzite pebbles, and Liritzis [22] did likewise to obtain grains from the formerly sun-bleached surfaces of limestone blocks used to construct megalithic buildings; both studies then derived doses using multiple-grain methods. Extension to other samples in which some constituent grains have been partially bleached or heated, or in which grains are too sparse for multiple-grain analysis, would be practical and advantageous if a reliable method of measuring the $D_e$ in single grains was available.

## 2. True single-aliquot dating protocols

Until recently, the most rigorous protocol available for the dating of a single-aliquot sample was that used for quartz [12]. Duller [23] proposed an additive-dose protocol based on infrared stimulated luminescence (IRSL) measurements following repeated laboratory doses on a single feldspar aliquot but he required a second aliquot to calibrate the decrease in the trapped electron population caused by the measurement process. He has since elaborated on this calibration procedure [24,25]. True single-aliquot procedures have been developed more recently.

Galloway [4] showed that the decay of IRSL in feldspar with $n$ repeated measurement cycles could be represented by the function $f(n) = 1 - a\ln(n)$, where $a$ is a constant. After measurement of an additive-dose growth curve, he used repeated IRSL measurements on the same aliquot without further laboratory dosing to define the calibration curve appropriate to that aliquot. Murray et al. [5] applied a related strategy to quartz; they showed that the calibration function was adequately represented by exponential decay, whose decay constant could also be measured at the end of a growth curve measurement sequence. They extensively tested this protocol on 14 samples covering the $D_e$ range 0.01–100 Gy, and demonstrated excellent agreement with the results of conventional multiple-aliquot measurements. Murray and Roberts [26] have developed a more rigorous form of the simple regenerative-dose procedure [12,13]. They repeatedly regenerated the OSL signal using a laboratory dose, and used the regenerated 110°C TL signal to correct for any non-linear sensitivity change with regeneration cycle. All three of these protocols are suitable, in principle, to the measurement of single-aliquots of arbitrary size, including single grains.

This paper makes use of the procedures described in [5,26] to look at the dose distribution in single

grains of quartz from a known-age aeolian sediment, which we consider to have been thoroughly bleached before deposition. We first test the suitability of the two single-aliquot protocols for the estimation of the $D_e$ in multiple-grain single aliquots of quartz from this sample. These protocols are then applied to individual quartz grains, and the resulting dose distributions discussed in terms of bleaching history and microdosimetry. The interpretation of multiple-grain luminescence characteristics is also considered in the light of the observed single-grain behaviour.

## 3. Site and sample descriptions

It is very important when testing new protocols that every effort should be made to use a well bleached sample of known age. We have selected aeolian sand-sized quartz from the archaeological deposit at Allen's Cave, located on the semi-arid Nullarbor Plain in southern Australia. The nature of the deposit makes it likely that the material was well bleached at deposition, and there is independent chronological evidence from $^{14}C$ and conventional luminescence dating which constrains the age of the chosen stratum.

Allen's Cave is a small rock shelter formed beneath an overhang in a shallow collapsed sinkhole developed in limestone. Five metres of quartz-rich wind-blown material has accumulated in the shelter, together with limestone blocks and other rubble collapsed from the bedrock walls. Fig. 1 presents a simplified stratigraphic section of the deposit (based on [27]) showing the sampling locations. Preliminary OSL and TL dates for the samples at 1, 150 and 390 cm have been published previously [27]; the revised dates given in Table 1 are only marginally altered. The dates at 265 and 470 cm are previously unpublished, and the dosimetry of the site is considered in detail elsewhere [28].

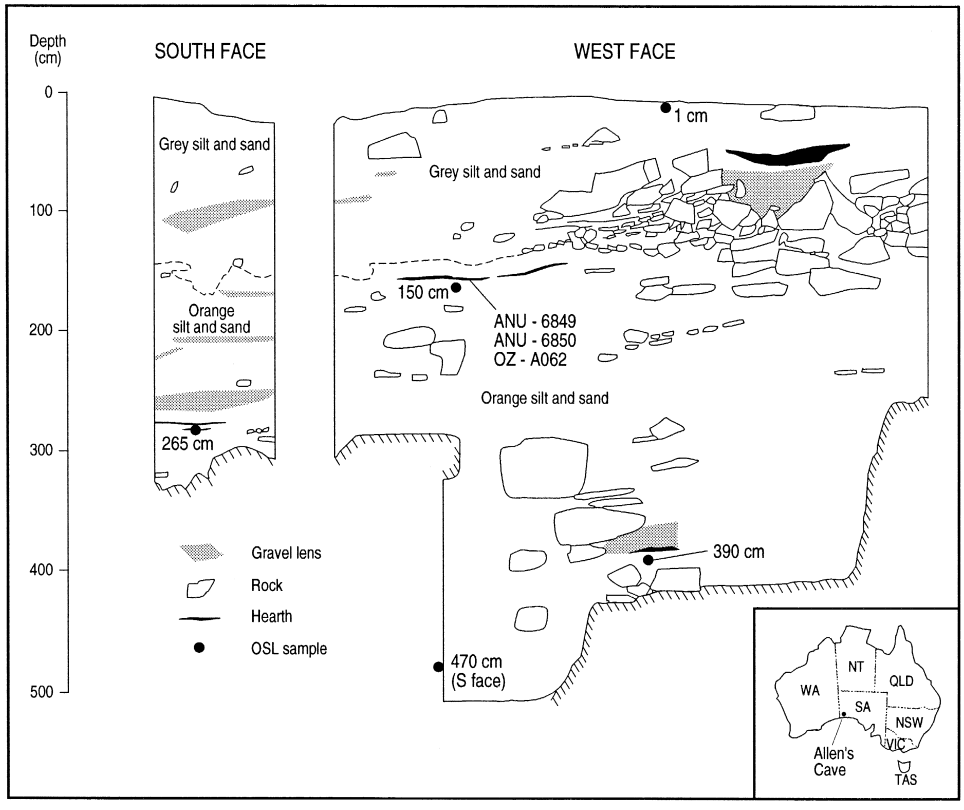


Fig. 1. Simplified stratigraphic section of the Allen's Cave deposit, showing OSL sample locations and the relative position of the $^{14}C$ dated charcoal.

Table 1
Summary of multiple-aliquot luminescence and calibrated $^{14}C$ dates for Allen's Cave

| Depth (cm) | Date (ka) | Type | Lab. code |
|---|---|---|---|
| 1 | $0.21 \pm 0.03$ | OSL | AC1 |
| 150 | $10.1 \pm 0.5$ | OSL | AC150 |
| 150 | $11.1 \pm 0.8$ | TL | AC150 |
| 145 | 10.5 (10.2–10.9) | $^{14}C$ | ANU-6849 |
| 145 | 10.2 (10.0–10.4) | $^{14}C$ | ANU-6850 |
| 145 | 10.0 (9.2–11.0) | $^{14}C$ | OZ-A062 |
| 265 | $16.2 \pm 1.0$ | OSL | AC265 |
| 390 | $39.6 \pm 2.6$ | OSL | AC2390 |
| 470 | $47.0 \pm 3.6$ | OSL | AC470 |

Calibrated $^{14}C$ dates expressed as mean age ($1\sigma$ age range), calibrated using CALIB 3.0 with the southern hemisphere correction [29].
Luminescence age uncertainties include both systematic and random components, and are $1\sigma$.

The sample used in this work was taken from 150 cm, 5 cm below a well preserved hearth; there is no evidence that this hearth was deeply excavated into an older surface, or that significant heating of the underlying sample has occurred. Three charcoal samples recovered from the hearth were dated using $^{14}C$ methods [27]; the calibrated dates [29] are given in Table 1. The three dates give a weighted average of $10.2 \pm 0.2$ ka for the age of the hearth, which puts an effective younger limit on the possible age of AC150.

Several lines of evidence suggest that this sample was well bleached when deposited:

1. All the quartz sand deposited in Allen's Cave must have travelled sub-aerially from its source to its ultimate deposition site, and thus have been exposed to direct sunlight, because the rock shelter walls and ceiling, and the bedrock in the vicinity of the site, are made of limestone.
2. The quartz grains were deposited on the floor of a rock shelter which receives direct insolation and has been a site of human habitation for the last 40 ka [27]. The rate of accumulation of Pleistocene material at this site is 3.2 m in 37 ka, or an average of 86 $\mu$m $a^{-1}$. Thus, any 100 $\mu$m diameter grain will have lain on the surface, on average, for more than a year before being buried. (Although individual sedimentation events must have deposited at a greater rate in the short term.) Construction of the hearth 5 cm above the level of AC150 sealed this sample from further disturbance, as testified by the well preserved appearance of this hearth.
3. The natural TL glow curve of this sample [5] shows that it is dominated by the easy-to-bleach 325°C TL peak, which is closely related to the source of the OSL signal in quartz [30,31]. This suggests that readily bleached luminescence signals are likely to be important in the OSL response.
4. The TL $D_e$ plateau for this sample extends over the temperature range 265–380°C, indicating that the hard-to-bleach 375°C TL peak was reset in antiquity to the same relative initial level as the 325°C TL peak [27].
5. The near-surface sample at Allen's Cave (AC1, Fig. 1) yielded a near-modern OSL age ($210 \pm 30$ yr) and a small $D_e$ ($0.35 \pm 0.05$ Gy [27]), consistent with being well bleached at deposition.
6. The OSL and TL multiple-aliquot dates for sample AC150 ($10.1 \pm 0.5$ ka and $11.1 \pm 0.8$ ka, respectively) are in close agreement with the independent $^{14}C$ age control for the overlying 10 ka hearth, indicating that there is no systematic overestimation of OSL age for the bulk sample due to incomplete bleaching in antiquity.

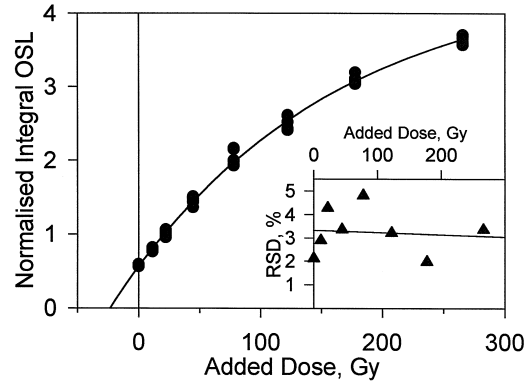


Fig. 2. Multiple-aliquot additive-dose OSL growth curve, fitted to 10 natural aliquots and 6 aliquots at each added dose. The data have been normalised to the OSL from a short light exposure made prior to the addition of laboratory doses. The saturating exponential fit (solid line) gives $D_e = 23.5 \pm 0.6$ Gy. The relative standard deviation (RSD; standard deviation divided by mean), expressed as a percentage, is shown inset as a function of added dose.

7. The relative scatter in the multiple-aliquot growth curve data points shows no correlation with added dose (see Fig. 2), as would be predicted if some grains on each aliquot had been incompletely bleached at deposition [14,32].

We conclude that sample AC150 cannot be younger than the overlying $10.2 \pm 0.2$ ka hearth. The multiple-aliquot OSL and TL dates from AC150 itself imply that the sample is unlikely to be older than the weighted mean of $10.3 \pm 0.5$ ka. Averaging the $^{14}C$ and multiple-aliquot luminescence dates provides the most likely deposition date for AC150, of $10.2 \pm 0.2$ ka.

## 4. Experimental facilities and sample preparation

All the single-aliquot (both multiple-grain and single-grain) experiments were carried out using an automated Risø TL/OSL reader with an OSL attachment [33]. The stimulating blue–green light source is a tungsten–halogen lamp filtered to 420–550 nm using a GG-420 filter in combination with an interference filter to reduce the scattered light reaching the Thorn-EMI 9235QA photomultiplier tube; this delivers about 13 mW $cm^{-2}$. The OSL is detected through an HA-3 and two 3 mm thick U340 filters. Experiments were run using Risø software, version 4.65. The reader is also equipped with a $^{90}Sr/^{90}Y$ beta source delivering 0.022 Gy $s^{-1}$ to 100 μm diameter grains of quartz loaded on 10 mm diameter stainless-steel discs.

The multiple-aliquot analysis employed the 514.5 nm (green) line from an argon-ion laser for optical stimulation ($\sim$ 12.5 mW $cm^{-2}$ delivered to the sample). Luminescence was detected through Corning 7-51 and Schott BG-39 filters using a Thorn-EMI 9635Q photomultiplier tube, and modified Elsec 9010 unit and software [27].

All sample processing was undertaken in subdued red ($>$ 590 nm) light. The sample was treated with hydrogen peroxide to oxidise organic material, hydrochloric acid to dissolve carbonates, and fluorosilicic acid and fluoboric acid to remove feldspars and micas. Heavy minerals were removed by density separation using solutions of sodium polytungstate. The residual quartz grains of 90–125 μm diameter were isolated by dry sieving and finally etched in 40% hydrofluoric acid for 45 min. All multiple-grain and single-grain samples were mounted on 10 mm diameter stainless-steel discs using silicon oil spray.

## 5. Measurement of $D_e$ using multiple-grain single-aliquots of quartz

Two single-aliquot protocols are used in this paper: additive-dose [5] and regenerative-dose [25]. The application and suitability of both of these protocols is first demonstrated using aliquots that each contain about 1 mg ($\approx$ 700 grains) of 90–125 μm diameter quartz.

### *5.1. Additive-dose single-aliquot protocol*

In this protocol, the intention is to define a dose-response curve by sampling the light-sensitive trapped electron population between successive laboratory doses, using an optical stimulation that is small enough to leave the trapped population essentially unaffected. However, some thermal treatment (the 'preheat') is applied prior to each OSL measurement, to mimic the redistribution of trapped charge during burial. The cumulative effect of this preheating and subsequent optical stimulation is to reduce significantly the electron population in the traps of interest, and so some correction for this decrease must be made. A full description of this approach is given in [5].

Fig. 3a presents a data set obtained using the additive-dose single-aliquot protocol. This sample was first preheated at 5°C $s^{-1}$ to 280°C, and held there for 10 s. It was allowed to cool to room temperature before being heated to 125°C and exposed to blue–green light for 0.1 s at that temperature to measure the OSL. It was then given a laboratory beta dose, and the preheat and measurement cycle repeated. This dose/preheat/measurement cycle was repeated a further 4 times, and the OSL signals observed are shown in Fig. 3a (as circles) in the cumulative added dose range 0–50 Gy. The sample was then preheated again (without the addition of further dose) and the OSL measured as before, this treatment was repeated a further 4 times, and the data are also shown in Fig. 3a as circles, plotted against stimulation cycle. The OSL signal

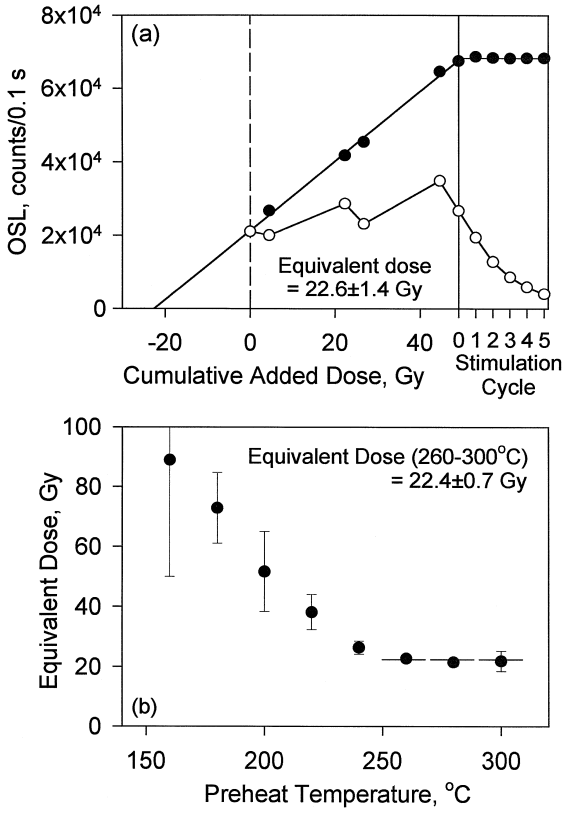


Fig. 3. (a) Application of the single-aliquot additive-dose protocol to a multiple-grain sample of AC150. ○ = raw data; ● = data corrected using the average exponential decay of the last 5 raw data points. Note that the cumulative added dose increases only for the first 6 points. Thereafter, the sample was preheated (at 280°C for 10 s) and stimulated (0.1 s at 125°C) as before, but no further dose was added. The intercept on the dose axis gives the estimate of $D_e$ ($22.6 \pm 1.4$ Gy). (b) Variation of apparent $D_e$ with preheat temperature. All aliquots were held for 10 s at the relevant temperature before cooling to room temperature. $D_e$ values from preheats of 260–300°C are indistinguishable.

observed during the latter treatment decayed approximately exponentially, and the average decay rate (38% per cycle) has been used to correct all the data points for loss of OSL signal [5]. The corrected data are shown as dots, and it can be seen that this cumulative correction procedure has satisfactorily corrected for the (average) decrease in the OSL signal in the last 5 data points. After correction, the first six OSL measurements form a linear growth curve, which can be extrapolated back to the dose axis (instrument noise is negligible), to provide a $D_e$ estimate of $22.6 \pm 1.4$ Gy. Note that the added doses were given in unequal increments to test for sensitivity changes during measurement [5]. No such changes were detected.

The preheat regime adopted must be sufficient that electrons trapped during a laboratory dose are redistributed in a similar manner to the redistribution which occurred in the sample during burial. This was checked by investigating the effect on the apparent $D_e$ of using preheat temperatures of between 160°C and 300°C (with each aliquot held for 10 s at the relevant temperature), and determining the temperature range over which $D_e$ remained constant (a 'preheat plateau', see [5,8,34]). These data (averages and standard errors of triplicates) are presented in Fig. 3b, in which the apparent $D_e$ becomes constant for preheats above about 250°C. Accordingly, a preheat temperature of 280°C was adopted for all subsequent analyses. Preheats above 300°C cannot be used because thermal erosion of the OSL signal becomes unacceptably large. Thermal erosion from 280°C preheats is the main cause of the signal decrease in the last 5 uncorrected data points in Fig. 3a. The average $D_e$, from 260°C to 300°C, is given in Table 2.

### 5.2. Regenerative-dose single-aliquot protocol

In the regenerative-dose approach, the natural OSL is measured, the sample is given a laboratory dose,

Table 2
Summary of $D_e$ estimates obtained using protocols for multiple (M) and single (S) aliquots composed of multiple grains, and single-aliquot protocols for individual grains (Sg)

| Protocol | | m [a] | n [b] | Grains in aliquot | $D_e$ (Gy) |
|---|---|---|---|---|---|
| Additive-dose | S | 1 | 9 | ~ 700 ( ~ 1 mg) | $22.4 \pm 0.7$ |
| Regenerative-dose | S | 1 | 13 | ~ 700 ( ~ 1 mg) | $23.9 \pm 0.3$ |
| Additive-dose (OSL) | M | 52 | 1 | ~ 4000 ( ~ 5 mg) | $23.5 \pm 0.6$ |
| Additive-dose (TL) | M | 43 | 1 | ~ 4000 ( ~ 5 mg) | $25.9 \pm 1.4$ |
| **Weighted average** | | | | | $23.7 \pm 0.3$ |
| Additive-dose | Sg | 1 | 28 | 1 | $21.8 \pm 1.1$ |
| Regenerative-dose | Sg | 1 | 25 | 1 | $23.8 \pm 1.0$ |
| **Weighted average** | | | | | $22.7 \pm 0.8$ |

[a] The number of aliquots used for each estimate of $D_e$.
[b] The number of independent estimates of $D_e$.

and the OSL measured again. The total OSL signal (rather than the initial signal) is measured during each cycle, so that prior to any laboratory dose there is essentially no light-sensitive trapped electron population. In the absence of sensitivity changes, $D_e$ can then be calculated from the ratio of the natural and regenerated OSL signals, and a knowledge of the laboratory dose used to regenerate the OSL signal [12,13]. This dose should be chosen to match as closely as possible the natural dose, to minimise the effects of any non-linearity in the OSL dose-response curve. In practice, significant sensitivity changes often occur and these are usually non-linear with repeated regeneration dose. A reliable estimate of $D_e$ can only be obtained if due allowance is made for this sensitivity change.

Murray and Roberts [26] based a correction procedure on the 110°C TL signal obtained during the preheat given after each laboratory dose. They showed that sensitivity changes in this signal correlate with those in the OSL signal, and Wintle and Murray [31] also found the two signals to be strongly correlated. Changes in the 110°C TL signal are used as proxy measures of OSL sensitivity changes that have resulted from the laboratory treatments given with each regeneration cycle. The OSL signal measured in any particular cycle is corrected using the 110°C TL signal measured during the preheat which is given after the next (regeneration) dose. The correction is based on the observation that an OSL sensitivity change induced by blue–green light illumination and subsequent dosing is accompanied by a change in the 110°C TL signal measured during the following preheat [26]; differences in OSL sensitivity between successive cycles can then be eliminated by comparing the regenerated OSL in each cycle to the subsequently regenerated 110°C TL.

The regenerated OSL and TL signals obtained from a single aliquot of AC150 are shown in the inset in Fig. 4. The sample was first preheated to 280°C, held there for 10 s, and cooled to room temperature. The OSL was then measured during 100 s of blue–green light stimulation, with the sample held at 125°C. The net OSL signal was calculated by integrating the OSL signal over the full 100 s of stimulation and subtracting a background based on the average count rate observed during the final 10 s. The net natural OSL is shown as an open square in the inset, plotted against regeneration cycle 1. (Note the OSL results have been multiplied by 2 for comparison with the TL data.) The aliquot was then given a laboratory dose of 22.9 Gy (approximately equal to $D_e$) and preheated again. During this preheat, the TL signal in the 110°C peak was observed, and this is plotted as the closed triangle corresponding to regeneration cycle 1. This OSL/dose/TL measurement cycle was then repeated 7 times, and the regenerated OSL data are shown as closed squares, and the TL data as closed triangles. Saturating exponentials (with intercepts on the luminescence axis) have been fitted to allow extrapolation of the OSL data back to the first cycle. While it is possible to use such an extrapolation to predict the OSL that corresponds to a 22.9 Gy dose during the first cycle, and thus estimate the $D_e$, such an extrapolation is unacceptably dependent on the model used to fit the data. However, the shape of the TL curve is very similar to that fitted to the OSL data. In Fig. 4 the same natural and regenerated OSL (circles and dots, respectively) are plotted against the corresponding TL data; the relationship of the regenerated data

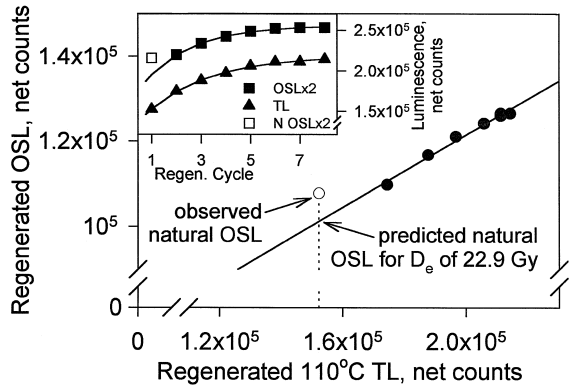


Fig. 4. Application of the single-aliquot regenerative-dose protocol to a multiple-grain sample of AC150. ● = regenerated data; ○ = natural OSL plotted against the first regenerated 110°C TL signal. The $D_e$ ($24.4 \pm 1.8$ Gy) is derived from the regeneration dose (22.9 Gy) multiplied by the ratio of the natural OSL signal to the OSL predicted at the same TL co-ordinate by extrapolation of the linear relationship between the regenerated OSL and TL signals. Inset are the OSL and 110°C TL signals plotted against regeneration cycle, with the natural OSL shown as an open square on the first cycle; the OSL signals have been multiplied by two so that the same scale can be used. Saturating exponentials have been fitted to the regenerated OSL and TL data.

is satisfactorily represented by a best-fit straight line. This line has been extrapolated back through the TL signal observed after measurement of the natural OSL; the ratio (1.064) of the natural OSL to the predicted OSL at this TL co-ordinate was multiplied by the regeneration dose (22.9 Gy) to estimate the $D_e$ ($24.4 \pm 1.8$ Gy).

This protocol has been used to estimate the $D_e$ in 13 aliquots, and the weighted average, $23.9 \pm 0.3$ Gy, is given in Table 2.

### 5.3. Discussion of multiple-grain analyses

The $D_e$ in this sample has also been measured using the multiple-aliquot additive-dose protocol for both OSL (using a preheat of 220°C for 300 s) and high temperature TL [27]. The results of these measurements are also summarised in Table 2. All values are in satisfactory agreement with a weighted mean of $23.7 \pm 0.3$ Gy. Dose rate data [27,28] have been used with this mean $D_e$ to calculate an age of $10.2 \pm 0.4$ ka, in excellent agreement with the mean of the three calibrated $^{14}C$ ages of $10.2 \pm 0.2$ ka for the immediately overlying hearth. This result gives confidence that the sediment was well bleached at deposition, and that the two independent single-aliquot protocols provide satisfactory estimates of the true $D_e$ in the bulk sample. These protocols can now be applied to single grains.

## 6. Measurement of $D_e$ using single grains of quartz

### 6.1. Additive-dose single-aliquot protocol

To test the application of the additive-dose approach, 120 single grains of quartz (90–125 μm diameter) of sample AC150 were each mounted, using silicon oil, on separate 10 mm diameter stainless-steel discs. Each grain was preheated at 280°C for 10 s, and then optically stimulated for 0.1 s at 125°C. The observed natural OSL signals ranged from 0 to 413 counts. It was found that 5% of the grains produced about 57% of the summed natural luminescence output of all 120 grains. This finding is comparable with the results of McFee and Tite [35], who examined the TL of single quartz grains using an imaging photon detector. For aeolian samples from four different sites, they found that 5% of the grains carried between 21% and 26% of the total natural TL.

We then continued the additive-dose single-aliquot measurements on those grains ($n = 33$) which gave 10 counts or more (cf. background of 0–1 counts) for the preheated natural. Only grains which gave exponential decay constant corrections with $R^2 \geq 0.8$ were considered acceptable. This led to the rejection of a further 5 grains (those with the lowest light levels), leaving 28 estimates of $D_e$ from individual

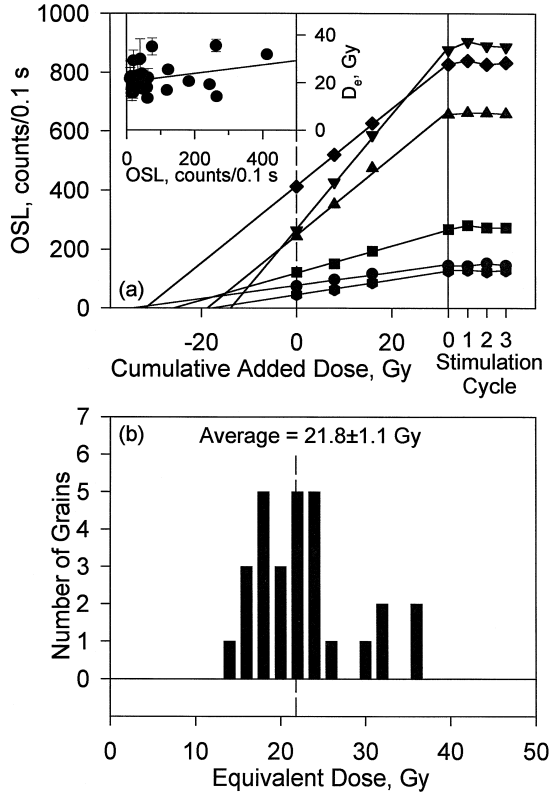


Fig. 5. (a) Single-aliquot additive-dose growth curves for 6 representative individual quartz grains. The first 4 data points on each curve constitute the growth curve; the last 3 points show the effect of correcting for the exponential decay which results from repeated preheat/stimulation without further added dose (see Fig. 3a). The extrapolated solid straight lines are best fits to the four decay-corrected growth curve data points for each grain. Note the good fits, and the wide range of natural OSL intensities and dose sensitivities. The $D_e$ values calculated from 28 such growth curves are compared with the corresponding natural OSL intensities in the inset figure. (b) Frequency distribution of single-aliquot additive-dose protocol estimates of $D_e$ from 28 individual quartz grains. The average value of $D_e$ is $21.8 \pm 1.1$ Gy, and the distribution has a standard deviation of 6 Gy.

quartz grains. A representative selection of 6 of these single-grain growth curves is shown in Fig. 5a, and a frequency distribution of all 28 $D_e$ estimates in Fig. 5b. The average of the distribution is $21.8 \pm 1.1$ Gy, within two standard errors of the average of the multiple-grain values ($23.7 \pm 0.3$ Gy; see Table 2).

However, the width of the dose distribution is noteworthy. The standard deviation is about 6 Gy, and the minimum and maximum $D_e$ observations are $13.5 \pm 1.5$ Gy and $36 \pm 3$ Gy, respectively. There is some suggestion that the distribution may not be uni-modal, but there are insufficient data to be certain. The range of values of $D_e$ is not related to grain brightness; there was no significant correlation ($R = 0.10$; Fig. 5a inset) between the values of $D_e$ and the natural OSL intensities, and the two largest natural OSL signals (413 and 265 counts) gave $D_e$ estimates of $31.9 \pm 0.5$ Gy and $14.2 \pm 0.6$ Gy, respectively.

### 6.2. Regenerative-dose single-aliquot protocol

A further 100 single grains were mounted on stainless-steel discs, and all were analysed using the regenerative-dose protocol described above, and a regeneration dose of 22.9 Gy. In this experiment, the instrument background became significant when measured over a period of 100 s. As a result, the net OSL signal was derived from the total OSL signal integrated over the first 30 s of stimulation (rather than 100 s as used for the multiple-grain analyses), and the background count rate was estimated from the 30–50 s interval. Consideration of counting statistics led to the adoption of a net OSL signal of 50 counts as a minimum detection limit. Of the 100 grains examined, 25 gave natural OSL signals above this level. Results from six individual grains are shown in Fig. 6a, and these illustrate the range of characteristics observed. Note that the natural and regenerated OSL signals from one grain (the brightest of the 100 examined) have been divided by 10 to facilitate comparison with the other signals; the TL values are unaltered. Four of the grains, including the brightest, behaved similarly to the multiple-grain aliquots described earlier. However, 2 grains (shown by diamonds and hexagons in Fig. 6a) displayed no significant TL sensitisation with regeneration cycle, and one grain (hexagons) also showed little OSL sensitisation. The slopes of the OSL/TL relationships vary considerably from grain to grain, demonstrating a variable response to identical laboratory treatments. An estimate of $D_e$ has been obtained for each grain, and these are presented (in Gy) adjacent to each data set; as before, there is no correlation between $D_e$ and net natural OSL intensity ($R^2 = 0.005$; Fig. 6a inset).

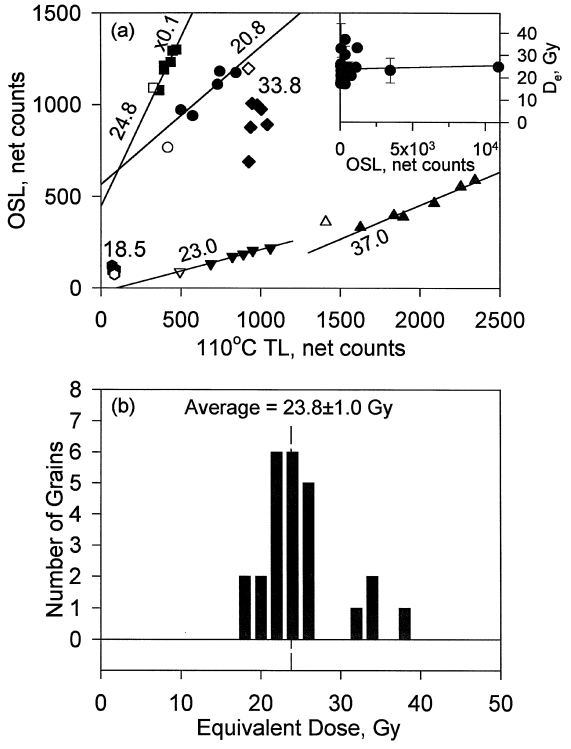


Fig. 6. (a) Single-aliquot regenerative-dose OSL/TL curves for six representative individual quartz grains. The natural OSL signals are represented by open symbols, and the regenerated data by closed symbols. Where shown, the straight lines are best fits to the regenerated data only. The values of $D_e$ (Gy), calculated as described in the text and in Fig. 4, are shown adjacent to each data set. The OSL (but not the TL) data, represented by closed and open squares, have been divided by 10 so the same scale can be used. Note the wide range of absolute OSL and TL sensitivities, relative sensitivity changes, and OSL/TL ratios. $D_e$ values calculated for 25 single grains are compared with the corresponding natural OSL signals in the inset. (b) Frequency distribution of single-aliquot regenerative-dose estimates of $D_e$ from 25 individual quartz grains. The average value of $D_e$ is $23.8 \pm 1.0$ Gy, and the distribution has a standard deviation of 5 Gy.

Fig. 6b presents all 25 $D_e$ estimates as a frequency distribution. The possibility of a bi-modal distribution is more marked in these data than in the

additive-dose data set, probably because the main peak appears better resolved. The average of the distribution is $23.8 \pm 1.0$ Gy, with a standard deviation of 5 Gy. This accords with the average $D_e$ of the additive-dose single-grain results, and also with the best estimate of the multiple-grain $D_e$ derived in Table 2. Note that the estimate of $D_e$ is not biased by grain sensitivity within this sample of 25 grains. This also applies to the single-grain additive-dose protocol, but is contrasts with the multiple-grain $D_e$ estimates which must be heavily weighted towards the $D_e$ in the brightest grains.

### 6.3. Discussion of single-grain analyses

Lamothe et al. [9] discuss a similar but smaller data set for single grains of feldspar from a known age ($\sim$ 10 ka) marine deposit; their fifteen $D_e$ estimates were obtained using Duller's [23] additive-dose protocol. They observed a wide range in $D_e$, from $+690\%$ to $-30\%$ of that expected from the $^{14}C$ age, and concluded that the overestimates of $D_e$ were most likely to arise from incomplete bleaching, and the underestimates from anomalous fading. (As with Li's measurements on incompletely bleached feldspars [10], Lamothe et al. [9] required two grains for each $D_e$ estimate, with each grain possibly having a different bleaching and/or fading history).

In our sample, the average value of $D_e$ from 53 individual grains, obtained using 2 independent protocols, is $22.7 \pm 0.8$ Gy (see Table 2); the corresponding frequency distribution is shown in Fig. 7. (Note that the average is unweighted, because the individual estimates of uncertainty were significantly smaller than the spread in the data.) This average $D_e$ gives an age of $9.8 \pm 0.5$ ka, which is consistent with the mean (calibrated) $^{14}C$ age of $10.2 \pm 0.2$ ka [27].

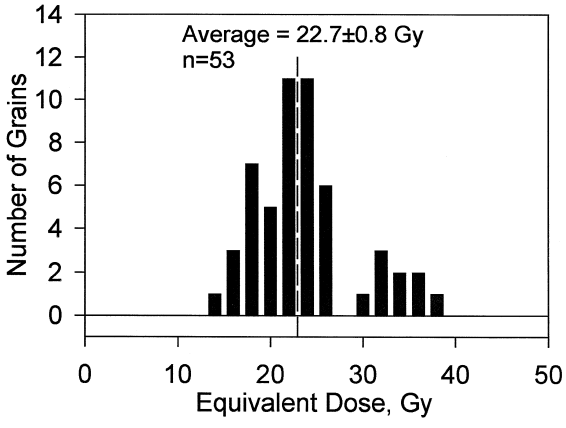


Fig. 7. Combined $D_e$ frequency distribution using the data of Fig. 5b and Fig. 6b.

## 7. Causes of $D_e$ distributions for individual grains from a single sample

In a well bleached deposit one might expect a dose distribution dominated by analytical uncertainties; as discussed above, this is not the case here. The width of the distribution in Fig. 7 is both unexpected and interesting. We will now discuss some potential causes of such variations.

### 7.1. Anomalous fading

Anomalous fading, as described for feldspars [8,18], would result in a reduction in apparent $D_e$. However, this phenomenon has never been reported in quartz luminescence studies. Given the agreement of the average single-grain OSL age with the mean calibrated $^{14}C$ age, fading can only be entertained as an explanation if, at the same time, some other phenomenon enhances the apparent $D_e$. The most obvious candidate for this would be incomplete bleaching at deposition but this is dismissed for the reasons given above. Moreover, anomalous fading tests on multiple-grain aliquots of sample AC150 showed no evidence of fading after 70 days storage at room temperature [27]. Anomalous fading is not, therefore, considered as a likely explanation for the observed $D_e$ distribution.

### 7.2. Thermal transfer

Various authors (e.g. [16,31,36]) have observed that the quartz OSL signal can be increased by preheating. This is usually attributed to thermally induced charge transfer from light-insensitive traps (thermally stable during burial) to the OSL trap. Such observations may also be partly explained by changes in the probability of an electron/hole recombination producing a detectable photon [26]. If optically insensitive traps contained a large dose at deposition, thermal transfer could be considerable (especially on younger samples), and variations in

the degree of transfer could contribute to our observed $D_e$ distributions. There are three reasons why we think this phenomenon is not important in our sample. First, the values of $D_e$ from all the multiple-aliquot and single-aliquot OSL measurements provide dates that are in excellent agreement with the average $^{14}C$ date of $10.2 \pm 0.2$ ka. Thermal transfer would have made the OSL dates systematically too old, rather than distribute them about the true value. Second, the multiple-aliquot date of $210 \pm 30$ yr for the near-surface sample (AC1) puts an upper limit to the significance of thermal transfer for this young sample.

Third, as a direct test of the importance of thermal transfer in sample AC150, we have measured a thermal transfer correction for natural aliquots. The net OSL signal (100 s stimulation) from a natural aliquot was measured at 125°C, but without any prior heat treatment. The aliquot was then preheated at 5°C $s^{-1}$ to 280°C and held at that temperature for 10 s, before remeasuring the net OSL as before. The preheat should transfer electrons from optically insensitive traps into the OSL trap (which at this time is empty, because of the first stimulation). The average ratio of the second/first OSL integral (3 aliquots) was $0.0085 \pm 0.0013$. The same experiment was repeated using a 220°C preheat for 300 s (as used in [27]), and the average ratio (3 aliquots) was $0.0478 \pm 0.0018$. These ratios place upper limits on the size of thermal transfer because no allowance has been made for sensitivity increases [26]. We conclude that, on average, the thermal transfer correction in AC150 is $< 1\%$ for the preheat used here, although it may be somewhat larger for the alternative preheat used to obtain the multiple-aliquot OSL dates [27]. Thus, thermal transfer cannot account for the below-average values in the $D_e$ distribution in Fig. 7, and so is dismissed as a significant contributor to the overall spread in $D_e$.

### 7.3. Remobilisation of buried sediment

Some reworking of buried sediment by human and faunal activity may have occurred prior to, or during, the construction of the hearth which overlies sample AC150. This could have resulted in some old sediment being brought close to the then surface. If this sediment was not exposed to daylight, the OSL signal would not be reset and the unbleached grains could be deemed to be responsible for the postulated bi-modal $D_e$ distribution in Fig. 5b, Fig. 6b and Fig. 7. The 10 Gy difference between the two $D_e$ modes requires that the reworked component be derived from sediments deposited at least 5 ka earlier. Using the average sedimentation rate quoted above, such grains would have to have been derived from depths of 40 cm or more below the level of AC150; using instead the OSL date of $16.2 \pm 1.0$ ka for sample AC265 (see Table 1), such grains would have to originate from at least 90 cm below AC150. Studies of artefact displacement in sandy deposits (e.g. [37,38]) indicate that stone tools can migrate upwards by 20–40 cm. Soil fauna (e.g. earthworms, termites, ground-nesting wasps and bees) can also can also mix deposits, both upward and downward, over such vertical distances (e.g. [39]), while large burrowing animals can redistribute substantial volumes of sediment [40]. Animal burrows were identified elsewhere in the Allen's Cave deposit from their preserved outline and contrasting infill, but none were apparent at the collection point of sample AC150. The horizontal to sub-horizontal bedding at this point, and the integrity of the pollen grain stratigraphy at this site [41], provide additional evidence that no gross disturbance has occurred at the sample location.

We cannot discount the possibility that soil fauna have been responsible for grain remobilisation on a small scale, resulting in some unbleached grains being mixed with an otherwise totally bleached sample. However, any form of vertical mixing by processes which simulate diffusion would be expected to give rise to a $D_e$ distribution with a long 'tail' towards higher doses, rather than a discrete subpopulation of grains. (A long 'tail' towards lower doses, due to the incorporation of grains derived from younger sediments overlying AC150, is not expected in this instance because of the seal provided by the intact hearth.) In our view, therefore, there are more credible reasons for the spread in $D_e$ values, and these are discussed below.

### 7.4. Variations in microdosimetry

Olley et al. [28] have considered the environmental dose rate at this site in detail, and the reader is

referred to the radionuclide concentrations and dosimetry calculations presented there. Because of the different ranges of alpha and beta particles, and gamma rays, it is most likely that any dosimetry variations from grain to grain reside in the beta and internally derived alpha dose rate. The average dose rate included an internal alpha and beta component (deduced from neutron activation analysis and thick-source alpha counting of the etched quartz grains) of 1.2% of the total dose rate. Thus, if the internal dose rate was reduced to zero, the mean age would increase only by 1.2%. It is more difficult to put bounds in the other direction, as grain-to-grain variations in the internal alpha and beta dose rate have not been investigated previously for individual quartz grains.

In an attempt to deal with this, we have determined the uranium and thorium concentrations in four of the 'bright' and four of the 'dim' grains of the 28 used to derive Fig. 5b; these analyses used laser-ablation inductively-coupled plasma mass-spectrometry [42], with a pulsed ArF excimer laser operating at 193 nm. This technique allows examination of elemental concentrations as a function of time, as the laser ablates the surface of a grain. The maximum U and Th concentrations for each grain are given in Table 3. Only two grains had localised concentrations in excess of the minimum detection limits of approximately 0.015 ppm U and 0.022 ppm Th. Using an assumed alpha efficiency a value of 0.1 [43], the absorbed beta dose fractions for 100 $\mu$m diameter quartz grains given in [44], and published dose rate conversion factors [45], we calculate that the maximum internal (U plus Th) dose rate at a point ranges from $< 0.006$ to 0.9 Gy ka$^{-1}$ in the 8 grains examined. In the grain with the highest observed concentrations, the concentration peak was only detected over a period of 1 s, compared with a total ablation time of 60 s; this suggests an average internal dose rate for the grain of about 0.015 Gy ka$^{-1}$, compared with the total dose rate of about 2.3 Gy ka$^{-1}$. It is also clear from Table 3 that the $D_e$ values are not related to the maximum U and/or Th concentrations, and we conclude that variations in microdosimetry arising from internal U and Th radioactivity are insufficient to explain the spread in $D_e$ estimates shown in Fig. 5b.

It is possible that potassium feldspar inclusions within the grains could give rise to a locally significant beta dose from $^{40}$K decay. A means of testing for feldspar inclusions is to stimulate with infrared radiation because some feldspars, but not quartz, produce IRSL at room temperature [8,30]. In multiple-grain measurements, however, Roberts et al. [27] found that the natural IRSL signal in sample AC150 was at least $10^5$ times smaller than the natural OSL signal (stimulated using the 514.5 nm line from an Ar-ion laser). We have repeated this measurement, using the IRSL signal regenerated after a laboratory dose of 70 Gy, and the corresponding OSL signal excited by 420–550 nm light, and obtained similar results. Although these observations are not conclusive, it is thought very unlikely that there are significant feldspar inclusions within these grains.

Two external sources of heterogeneity due to microdosimetry should also be considered: small-scale variations in water content, and local dose rate variations arising from the proximity of minerals of different radioactivity. Local porosity variations in a deposit would give rise to differences in local water

Table 3
Maximum U and Th concentrations in eight individual quartz grains of sample AC150

| Grain | Natural OSL counts/0.1 s | Single-aliquot $D_e$ (Gy) | Max. U conc. (ppm) | Max. Th conc. (ppm) |
|---|---|---|---|---|
| 1 | 265 | $14.2 \pm 0.6$ | $< 0.015$ | $< 0.022$ |
| 2 | 183 | $20.6 \pm 1.3$ | $< 0.015$ | $< 0.022$ |
| 3 | 122 | $25.5 \pm 1.3$ | $< 0.015$ | $< 0.022$ |
| 4 | 413 | $31.9 \pm 0.5$ | 0.091 | $< 0.022$ |
| 5 | 15 | $16 \pm 2$ | $< 0.015$ | $< 0.022$ |
| 6 | 16 | $22 \pm 3$ | $< 0.015$ | $< 0.022$ |
| 7 | 20 | $29 \pm 4$ | 0.23 | 10.3 |
| 8 | 75 | $35 \pm 4$ | $< 0.015$ | $< 0.022$ |

content. The mean water content used to calculate the dose rate for sample AC150 was $5 \pm 2\%$. Reducing this value to zero increases the dose rate by only 5.7%. The maximum local void is not known but, in any case, water content variations cannot explain the upper end of the range of observed values of $D_e$, and so can be dismissed as a probable sole cause of the $D_e$ distribution.

External variations in radioactivity over distances of a few millimetres cannot, however, be so easily dismissed. In their detailed study of the dosimetry at this site, Olley et al. [28] concluded that the 5 m thick cave deposit has an average composition, throughout its profile, of about 70% aeolian clay/silt/sand and 30% carbonate, the latter being derived from the weathering of the limestone sinkhole in which the deposit is situated. The carbonate fragments range in size from sand particles to spalled rubble and boulders. For a quartz grain surrounded by several millimetres of carbonate, the quartz would receive the site-average gamma and cosmic ray dose rate but all its beta dose from the carbonate; the resulting total dose absorbed by the grain would then be 60% lower than the bulk average [28]. Conversely, for a grain receiving all its beta dose from the aeolian material, the total dose received will be 70% greater than the bulk average. These microdosimetry variations are of the same order-of-magnitude as the range in $D_e$ values reported in Fig. 5b, Fig. 6b and Fig. 7.

### *7.5. Variations in luminescence response to laboratory treatment*

We must also consider the possibility that each grain responds differently to laboratory treatment, such that the multiple-grain single-aliquot luminescence signal (and any multiple-aliquot signal) is derived from the sum of signals from individual grains, each with a different sensitivity and different natural luminescence, as shown in Fig. 5a and Fig. 6a.

From the agreement between the multiple-grain single-aliquot additive-dose results and the independent age estimates, we can conclude that the linear extrapolation in Fig. 3a is justified over the applied dose range. This may not be true, however, for each grain considered separately. The effect of grain-to-grain differences in dose response on the $D_e$ obtained using the additive-dose protocol was tested directly by generating growth curves for individual grains of AC150 which had been optically bleached. First, 120 individual grains were mounted on stainless-steel discs, as described previously, but all handling was done in full daylight. Each grain was then given a 2.2 Gy test dose, and stimulated using a 0.1 s exposure to blue–green (420–550 nm) light. The brightest 24 grains were subsequently bleached thoroughly by further exposure to daylight and 200 s of blue–green light. The single-aliquot additive-dose protocol was then used to generate growth curves; five of these are shown in Fig. 8a to illustrate the different types of dose response observed. Note that only one grain (the brightest of those shown, with OSL intensities divided by 10 for presentation) has an approximately linear dose response; the other four grains show a variety of curve shapes. The two lowest intensity curves are sub-linear, while the two intermediate intensity curves may show regions of both supra-linear and sub-linear growth. To investigate the potential importance of this variation, the additive-dose points above 20 Gy were fitted with a straight line, which was then extrapolated to the dose axis; the negative dose intercepts ($D_o$) obtained by this procedure for all 24 grains are shown as a frequency distribution in Fig. 8b. The average value of $D_o$ is $2.8 \pm 1.0$ Gy, and the standard deviation is 5 Gy. This spread is comparable to that of the additive-dose $D_e$ data set shown in Fig. 5b. The $D_e$ values also are plotted against the luminescence observed at the 20.65 Gy cumulative dose points, in the inset to Fig. 8a. This figure corresponds to the inset to Fig. 5a and, as with the latter, there is no significant relationship ($R^2 = 0.008$) between the dose-axis intercept and the grain luminescence.

These results suggest that the observed distribution in $D_e$ values derived using the additive-dose protocol may arise from variations in the degree of supra-linearity or sub-linearity in the dose response of individual grains at small added doses; these variations are not necessarily reflected in the growth curve shape at higher doses. The results also imply that the shape of a multiple-grain growth curve is not an intrinsic dose-response characteristic of the quartz under investigation but, rather, is the arithmetic sum of many different growth curve shapes. If different

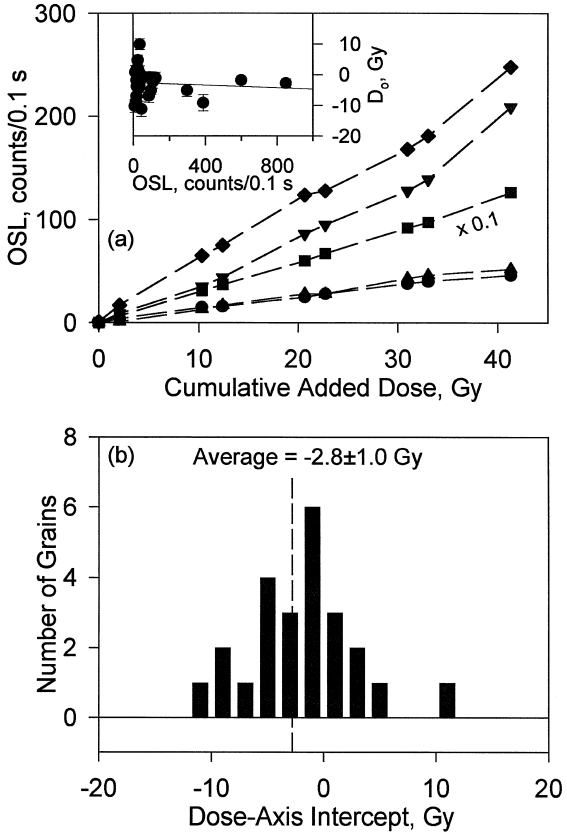


Fig. 8. (a) Single-aliquot additive-dose growth curves for 5 representative quartz grains (doses added after exposing grains to daylight and 200 s of 420–550 nm light). For presentation, the counts represented by closed squares have been divided by 10. For comparison with the additive-dose data shown in Fig. 5, the dose points above 20 Gy were fitted by a straight line which was extrapolated back to the dose axis. The negative dose-axis intercepts ($D_o$) calculated from 24 such growth curves are compared with the corresponding OSL intensities at the 20.65 Gy cumulative dose points in the inset. (b) Frequency distribution of single-aliquot protocol estimates of $D_o$ from 24 individual quartz grains, derived from extrapolated additive-dose growth curves as described in (a). The average value of $D_o$ is $2.8 \pm 1.0$ Gy, and the distribution has a standard deviation of 5 Gy.

growth curves saturate at different rates with respect to dose, the overall growth curve for a suite of grains may exhibit regions of linear and non-linear response as different types of individual growth curve dominate the luminescence output. (The fact that such behaviour may be observed in Fig. 8a, even for single grains, hints at further within-grain heterogeneity.) Various authors have observed such changes in the shape of additive-dose growth curves: in the IRSL of loess [46]; in the TL of fine-grained sediments [47]; and in the ESR signal from mollusc shell [48]. If multiple-grain OSL growth curves for quartz are indeed the sum of many curves of different shapes, then this has serious implications for attempts to model the dose-response characteristics of quartz based on observations from multiple-grain aliquots.

The regenerative-dose protocol, however, should not be sensitive to variations in the shape of the dose-response curve, because the regeneration dose returns the trapped electron population to a similar position along the trapped charge growth curve, regardless of its shape. Any non-linearity at low doses should, therefore, be irrelevant. Despite this apparent advantage, the regenerative-dose protocol produced a similar single-grain $D_e$ distribution to that obtained using the additive-dose protocol, although the regenerative-dose distribution appears to be slightly better resolved. It may be that this improved resolution arises from the elimination of the effects seen in Fig. 8.

Finally, there is the possibility that the $D_e$ distributions are a consequence of each grain responding differently to the given preheat (280°C for 10 s). We have shown (Fig. 3b) that this preheat is generally suitable for multiple-grain aliquots but we do not know if the same preheat results in identical charge redistribution within individual grains. If the chosen preheat causes complete thermal transfer of unstable charge in some grains and incomplete transfer and/or preheat-induced sensitivity change in others, then a distribution in $D_e$ could be expected. The situation becomes more complex if the electron traps involved in OSL production occur at more than a single trap depth [49]. We cannot examine these propositions directly because a preheat plateau test cannot be performed on a single grain. It seems unlikely, however, that preheat-related effects are the sole or principal cause of the observed spread in $D_e$ values, given the $< 1\%$ thermal transfer correction required for the multiple-grain aliquots (using the 280°C/10 s preheat) and given the demonstrated significance of variations in the microdosimetry and dose response of discrete grains.

We conclude that the width of the additive-dose and regenerative-dose single-grain $D_e$ distributions

(Fig. 5b, Fig. 6b and Fig. 7) can be explained by heterogeneity in the beta dosimetry, although the non-linear growth curves of some grains may augment the spread of the measured additive-dose distribution.

## 8. Conclusions

Both the additive-dose and regenerative-dose protocols have provided $D_e$ estimates for multiple-grain single aliquots of sample AC150 that are consistent with previously published multiple-aliquot additive-dose TL and OSL estimates, and with $^{14}C$ age determinations on charcoal pieces from an overlying hearth. We conclude that these protocols are reliable when applied to the bulk sample and, thus, by extension, to single grains of quartz from this sample. The average estimates of $D_e$, obtained from the application of the additive-dose single-aliquot protocol to 28 grains (out of 120, i.e. representing ~23% of the sample), and of the regenerative-dose single-aliquot protocol to 25 grains (out of 100, thus representing ~25% of the sample), are consistent with $D_e$ estimates based on both multiple-aliquot and single-aliquot multiple-grain analyses. The dose distributions are unexpectedly wide, however, with standard deviations of 27% and 21% of the mean. There is some suggestion that the distributions are bi-modal, with one peak (containing ~83% of the population) at about 23 Gy, and the other (~17% of the population) at about 34 Gy. We suggest that most of the spread in the distributions has arisen from heterogeneity in external beta dosimetry, although there may be a small additional contribution to the breadth of the additive-dose $D_e$ distribution from variable non-linearity in the low-dose regions of the growth curves of individual grains. It is also possible that the chosen preheat is responsible for some of the spread in $D_e$ values, and that bioturbation may account for the peak in the frequency distribution at ~34 Gy.

Individual grains show considerable variability in their OSL and TL characteristics in terms of their initial brightness and sensitivity to added dose, the rate of sensitivity change during dose regeneration, and the relationship between the regenerated OSL and 110°C TL signals. We conclude that the detailed luminescence characteristics of a typical 5–10 mg (~4000–7000 grains) aliquot are the arithmetic sum of many different individual grain behaviours and do not represent any fundamental physical characteristics of quartz, other than at the gross level.

This study has revealed a pattern in the distribution of $D_e$ which could not have been obtained without the new single-aliquot protocols. We find this advance very encouraging, and envisage that such protocols will allow reliable luminescence ages to be obtained for a variety of Quaternary sediments that hitherto have proved difficult to date, especially those in which some constituent grains have been incompletely reset by light or heat before burial.

## Acknowledgements

We thank Jon Olley, Ann Wintle and Geoff Duller for helpful suggestions throughout this work, and for comments on the manuscript. Dave Huntley also provided a thorough and valuable review. Scott Cane and Rhys Jones assisted with sample collection, Malcolm McCulloch kindly granted access to the laser-ablation ICP–MS facility, and Mike Shelley and Les Kinsley are thanked for performing the U and Th analyses. Some of the equipment used in this study was purchased with the assistance of the Co-operative Research Centre for Catchment Hydrology. RGR is supported by a Queen Elizabeth II Fellowship from the Australian Research Council. *[FA]*

## References

[1] P.W. Layer, C.M. Hall, D. York, The derivation of $^{40}Ar/^{39}Ar$ age spectra of single grains of hornblende and biotite by laser step-heating, Geophys. Res. Lett. 14 (1987) 757–760.

[2] T.W. Stafford Jr., P.E. Hare, L. Currie, A.J.T. Jull, D.J. Donahue, Accelerator radiocarbon dating at the molecular level, J. Archaeol. Sci. 18 (1991) 35–72.

[3] F. McDermott, R. Grün, C.B. Stringer, C.J. Hawkesworth, Mass-spectrometric U-series dates for Israeli Neanderthal/early modern hominid sites, Nature 363 (1993) 252–254.

[4] R.B. Galloway, Equivalent dose determination using only one sample: alternative analysis of data obtained from infrared stimulation of feldspars, Radiat. Meas. 23 (1996) 103–106.

[5] A.S. Murray, R.G. Roberts, A.G. Wintle, Equivalent dose measurement using a single aliquot of quartz, Radiat. Meas. 27 (1997) 171–184.

[6] D.J. Huntley, D.I. Godfrey-Smith, M.L.W. Thewalt, Optical dating of sediments, Nature 313 (1985) 105–107.
[7] A.G. Wintle, D.J. Huntley, Thermoluminescence dating of ocean sediments, Can. J. Earth Sci. 17 (1980) 348–360.
[8] M.J. Aitken, Optical dating: a non-specialist review, Quat. Sci. Rev. (Quat. Geochronol.) 13 (1994) 503–508.
[9] M. Lamothe, S. Balescu, M. Auclair, Natural IRSL intensities and apparent luminescence ages of single feldspar grains extracted from partially bleached sediments, Radiat. Meas. 23 (1994) 555–562.
[10] S.-H. Li, Optical dating: insufficiently bleached sediments, Radiat. Meas. 23 (1994) 563–567.
[11] E.J. Rhodes, L. Pownall, Zeroing of the OSL signal in quartz from young glaciofluvial sediments, Radiat. Meas. 23 (1994) 581–585.
[12] A.S. Murray, J.M. Olley, G.C. Caitcheon, Measurement of equivalent doses in quartz from contemporary water-lain sediments using optically stimulated luminescence, Quat. Sci. Rev. (Quat. Geochronol.) 14 (1995) 365–371.
[13] J.M. Olley, G.C. Caitcheon, A.S. Murray, The distribution of apparent dose as determined by optically stimulated luminescence in small aliquots of fluvial quartz: implications for dating young sediments. Quat. Sci. Rev. (Quat. Geochronol.) (in press).
[14] G.A.T. Duller, Luminescence dating of poorly bleached sediments from Scotland, Quat. Sci. Rev. (Quat. Geochronol.) 13 (1994) 521–524.
[15] D.J. Huntley, G.W. Berger, Scatter in luminescence data for optical dating — some models, Ancient TL 13 (1995) 5–9.
[16] D.J. Huntley, J.J. Clague, Optical dating of tsunami-laid sands, Quat. Res. 46 (1996) 127–140.
[17] A.G. Wintle, S.-H. Li, G.A. Botha, Luminescence dating of colluvial deposits from Natal, South Africa, S. Afr. J. Sci. 89 (1993) 77–82.
[18] A.G. Wintle, Anomalous fading of thermoluminescence in mineral samples, Nature 245 (1973) 143–144.
[19] A.K. Singhvi, D. Banerjee, R. Rames, S.N. Rajaguru, V. Gogte, A luminescence method for dating 'dirty' pedogenic carbonates for paleoenvironmental reconstruction, Earth Planet. Sci. Lett. 139 (1996) 321–332.
[20] R. Roberts, G. Walsh, A. Murray, J. Olley, R. Jones, M. Morwood, C. Tuniz, E. Lawson, M. Macphail, D. Bowdery, I. Naumann, Luminescence dating of rock art and past environments using mud-wasp nests in northern Australia, Nature 387 (1997) 696–699.
[21] M.P. Richards, Luminescence dating of quartzite from the Diring Yuriakh site, M.A. Thesis, Simon Fraser Univ., 1994.
[22] I. Liritzis, A new dating method by thermoluminescence of carved megalithic stone building, C. R. Acad. Sci. Paris 319 (Sér. II) (1994) 603–610.
[23] G.A.T. Duller, Equivalent dose determination using single aliquots, Nucl. Tracks Radiat. Meas. 18 (1991) 371–378.
[24] G.A.T. Duller, Luminescence dating using single aliquots: new procedures, Quat. Sci. Rev. (Quat. Geochronol.) 13 (1994) 149–156.
[25] G.A.T. Duller, Luminescence dating using single aliquots: methods and applications, Radiat. Meas. 24 (1995) 217–226.
[26] A.S. Murray, R.G. Roberts, Measurement of the equivalent dose in quartz using a single-aliquot regenerative-dose protocol, Radiat. Meas. (submitted).
[27] R.G. Roberts, N.A. Spooner, R. Jones, S. Cane, J.M. Olley, A.S. Murray, M.J. Head, Preliminary luminescence dates for archaeological sediments on the Nullarbor Plain, South Australia, Aust. Archaeol. 42 (1996) 7–16.
[28] J.M. Olley, R.G. Roberts, A.S. Murray, Disequilibria in the uranium decay series in sedimentary deposits at Allen's Cave, Nullarbor Plain, Australia: implications for dose rate determinations, Radiat. Meas. 27 (1997) 433–443.
[29] M. Stuiver, P.J. Reimer, Extended $^{14}C$ data base and revised CALIB 3.0 $^{14}C$ age calibration program, Radiocarbon 35 (1993) 215–230.
[30] N.A. Spooner, On the optical dating signal from quartz, Radiat. Meas. 23 (1994) 593–600.
[31] A.G. Wintle, A.S. Murray, The relationship between quartz thermoluminescence, phototransferred luminescence, and optically stimulated luminescence, Radiat. Meas. (in press).
[32] E.J. Rhodes, Optical dating of quartz from sediments, D.Phil. Thesis, Oxford Univ., 1990.
[33] L. Bøtter-Jensen, G.A.T. Duller, A new system for measuring optically stimulated luminescence from quartz samples, Nucl. Tracks Radiat. Meas. 20 (1992) 549–553.
[34] E.J. Rhodes, Methodological considerations in the optical dating of quartz, Quat. Sci. Rev. 7 (1988) 395–400.
[35] C.J. McFee, M.S. Tite, Investigations into the thermoluminescence properties of single quartz grains using an imaging photon detector, Radiat. Meas. 23 (1994) 355–360.
[36] D.I. Godfrey-Smith, D.J. Huntley, W.-H. Chen, Optical dating studies of quartz and feldspar sediment extracts, Quat. Sci. Rev. 7 (1988) 373–380.
[37] D. Cahen, J. Moeyersons, Subsurface movements of stone artefacts and their implications for the prehistory of Central Africa, Nature 266 (1977) 812–815.
[38] P.J. Hughes, R.J. Lampert, Occupational disturbance and types of archaeological deposit, J. Archaeol. Sci. 4 (1977) 135–140.
[39] M. Armour-Chelu, P. Andrews, Some effects of bioturbation by earthworms (Oligochaeta) on archaeological sites, J. Archaeol. Sci. 21 (1994) 433–443.
[40] T.R. Paton, G.S. Humphreys, P.B. Mitchell, Soils: A New Global View, University College London Press, London, 1995.
[41] H.A. Martin, Palynology and historical ecology of some cave excavations in the Australian Nullarbor, Aust. J. Bot. 21 (1973) 283–305.
[42] W.T. Perkins, N.J.G. Pearce, T.E. Jeffries, Laser ablation inductively coupled plasma mass spectrometry: a new technique for the determination of trace and ultra-trace elements in silicates, Geochim. Cosmochim. Acta 57 (1993) 475–482.
[43] M.J. Aitken, Thermoluminescence Dating, Academic Press, London, 1985.
[44] V. Mejdahl, Thermoluminescence dating: beta dose attenuation in quartz grains, Archaeometry 21 (1979) 61–72.
[45] J.M. Olley, A.S. Murray, R.G. Roberts, The effects of disequilibria in the uranium and thorium decay chains on burial

dose rates in fluvial sediments, Quat. Sci. Rev. (Quat. Geochronol.) 15 (1996) 751–760.
[46] D.G. Questiaux, Optical dating of loess: comparisons between different grain size fractions for infrared and green excitation wavelengths, Nucl. Tracks Radiat. Meas. 18 (1991) 133–139.
[47] V. Mejdahl, Further comments on extrapolation methods of dating sediments by TL, Ancient TL 3 (1985) 21–26.
[48] O. Katzenberger, N. Willems, Interference encountered in the determination of AD in mollusc samples, Quat. Sci. Rev. 7 (1988) 485–490.
[49] D.J. Huntley, M.A. Short, K. Dunphy, Deep traps in quartz and their use for optical dating, Can. J. Phys. 74 (1996) 81–91.